

Original Research

YiQi ChuTan Recipe Inhibits Epithelial Mesenchymal Transition of A549 Cells under Hypoxia

C-M. Chen, L-L. Sun, R-M. Fang, L-Z. Lin*

Department of Tumor, the 1st Affiliated Hospital, Guangzhou University of Chinese Medicine, Guangzhou, China

Abstract: This study aims to investigate mechanism of YiQi ChuTan Recipe (YCR) for inhibiting epithelial mesenchymal transition (EMT) of A549 cells under hypoxia. Flow cytometry was used to optimize YCR dosage by measuring A549 apoptosis, which were subjected to different treatments, including normal condition, hypoxia, hypoxia+YCR. Cell morphology and expression of EMT were measured with differential interference contrast microscopy, real-time PCR and western blot. Optimized condition of 4 mg/ml YCR and 2% O₂ for 72 h was used to establish hypoxia. Under hypoxic condition, morphology of A549 cells changed from oblate fusi-form to elongated spindle. E-cadherin expression decreased while vimentin and fibronectin increased. EMT-related genes expression were significantly increased in hypoxia group compared to control group ($P < 0.05$). After treatment with YCR, mesenchymal cells obviously decreased and EMT-related genes expression was significantly decreased ($P < 0.05$). Changes of E-cadherin, vimentin and fibronectin were significantly attenuated by YCR when compared to hypoxia group. Expression of proteins GRP78, SRC, MAPK, smad2/3 were significantly increased in hypoxia group compared to control group, but was significantly inhibited by YCR treatment. In conclusion, A549 cells underwent EMT under hypoxia while YCR reversed the EMT through GRP78, smad2/3 and SRC/MAPK signal pathway.

Key words: Epithelial mesenchymal transition, YiQi ChuTan Recipe, A549, Hypoxia.

Introduction

The metastasis is a vital factor for the prognosis and a major factor for therapeutic failure and death in lung cancer which is a kind of malignant tumor with the highest mortality and morbidity in the world (1). Therefore, the prevention of lung cancer metastasis is a difficult problem. As a critical mechanism of tumor metastasis, epithelial-mesenchymal transition (EMT) has become the new hotspot for tumor study. EMT can increase the invasive and migrating capacities of tumor cells through multiple signals including mitogen-activated protein kinases (MAPK), tumor growth factor (TGF), and therefore contributes to tumor metastasis (2-4). Although there are large recent advancements in studying the mechanism of EMT, there is still no ideal therapeutic strategy for EMT and tumor metastasis.

Considering its bio-safety and mild effects, the Traditional Chinese Medicine (TCM) is receiving more and more attention in treating tumors (5,6). YiQi ChuTan Recipe (YCR) is an experiential TCM recipe, which could regulate the EMT pathway and the P4HB expression of A549 cells under hypoxia microenvironment (7). Previous study indicated that YCR could inhibit lung metastasis in implanted mouse model of Lewis lung carcinoma, down-regulated the expression of 18 proteins (particularly vimentin) in lung tissues with carcinoma (8). However, the detailed mechanism is not clear. In order to clarify the mechanism of YCR in treating metastatic lung carcinoma, the present study investigated the effects of YCR in EMT and related signaling pathway, particularly vimentin which is a key marker of EMT and plays critical role in the tumor metastasis (9).

Materials and Methods

Preparation of YCR

All herbal materials were purchased from the first Affiliated Hospital of Guangzhou University of Chinese Medicine, including pinellia ternate 15 g, American ginseng 30 g, pseudobulbus cremastrae seu pleiones 30 g and bulbus fritillariae thunbergii 15 g. The herbal materials were ground and filtered with 30-mesh sieve, decocted with decoction machine according to the manual and concentrated under 60°C to make YCR containing 2.0 g/ml raw material. The YCR was aliquoted, stored at -20°C, and diluted and filtered with 0.22 μm membrane before using.

Cell culture and treatment

Human lung adenocarcinoma A549 cells were purchased from the Cell Bank of the Chinese Academy of Sciences (Shanghai, China), and were cultured in RPMI-1640 medium (Gibco, USA) supplied with 10% FBS (Gibco, USA) and 100 U/ml penicillin/streptomycin in 5% CO₂ incubator at 37°C. The medium was changed every 3 days. The cells at logarithmic phase were used for experiments using different concentrations of oxygen at 1%, 2%, 5% and 10%. The cell morphology of was monitored daily under microscopy and the occurrence of obviously elongated fusiform mesenchymal cells was considered as establishment the hypoxia model. The condition was optimized as 2% O₂ and 72 h

Received October 21, 2015; Accepted January 01, 2016; Published January 11, 2016

* Corresponding author: Dr Li-Zhu Lin, Department of Tumor, the 1st Affiliated Hospital, Guangzhou University of Chinese Medicine, 16 Airport Road, Guangzhou 510405, China. Email: linleezh@yeah.net

Copyright: © 2016 by the C.M.B. Association. All rights reserved.

Table 1. Primers used in the study.

Primer	Gene ID on GenBank	Forwards	Reverse
Snail1	6615	15'-GCGAGCTGCAGGACTCTAAT-3'	5'-GGACAGAGTCCCAGATGAGC-3'
Snail2	6591	5'-GCCTCCAAAAAGCCAAACTA-3'	5'-CACAGTGATGGGGCTGTATG-3'
Twist	7291	5'-GCCGGAGACCTAGATGTCATT-3'	5'-CACGCCCTGTTTCTTTGAAT-3'
ZEB1	6935	5'-GCCAATAAGCAAACGATTCTG-3'	5'-TTTGGCTGGATCACTTTCAAG-3'
ZEB2	9839	5'-AAGCCAGGGACAGATCAGC-3'	5'-CCACACTCTGTGCATTTGAACT-3'
GAPDH	2597	5'-AACGGATTTGGTCGTATTGGGC-3'	5'-TTGATTTGGAGGGATCTCG-3'

for subsequent experiments.

The cells were treated differently, according to the following condition, including normal O₂ (control group), 2% O₂ (hypoxia group), 2% O₂+4 mg/ml YCR (YCR group).

Apoptosis measurement with Annexin V/PI

A549 cells were inoculated in 6-well plates and YCR was added at different concentrations as 4, 8 and 12 mg/ml for another 72 h. Each group set 3 repetition wells. Then the cells were collected and digested. A total of 1×10⁶ cells were collected from each well and added with Annexin V and PI solutions. Then, the cells were incubated in dark for 10 min followed by measurement with flow cytometry. In this experiment, in order to investigate whether a concentration of YCR at 4 mg/ml has any significant effect on A549 cells apoptosis, the statistical analysis was performed at least three independent experiments.

Real-time quantitative fluorescent PCR

After treatments, the cells were collected to extract total RNA using Trizol method. The cDNA was synthesized with PrimeScript™ RT Master Mix (RR036A; Takara, Japan) through reverse transcription and used as template to amplify target genes with real-time quantitative fluorescent PCR with SYBR® Premix Ex TaqII (RR820A; Takara, Japan). The primers (Invitrogen, USA) were listed in Table 1. The reaction condition was 95°C for 30 s, followed by 95°C for 5 s and 60°C for 30 s with 40 cycles. The amplified productions were quantitatively analyzed with 2^{-ΔΔCt} method.

Measurement of proteins with western blot

After treatment, the total proteins were extracted with RIPA buffer and quantified with BCA assay (Beijing Kangwei Biotech, China). 50μg total proteins were separated with 10% SDS-PAGE (Shanghai Beyotime Biotechnology, China), transferred to PVDF membrane (Millipore, USA), blocked with 5% BSA at room temperature for 1 h. The protein bands were cut according to the marker and added with primary antibodies, including mouse anti-human Fibronectin monoclonal antibody (sc-271098, 1:2000; Santa Cruz, CA, USA), mouse anti-human E-cadherin monoclonal antibody (sc-21791, 1: 2000; Santa Cruz, CA, USA), mouse anti-human Vimentin monoclonal antibody (sc-53464, 1: 1000; Santa Cruz, CA, USA), mouse anti-human PI3K monoclonal antibody (ab189403, 1:3000; Abcam, MA, USA), p-PI3K (catalogue number 3011, 1: 2000; Cell Signaling Technology, MA, USA), mouse anti-human AKT monoclonal antibody (sc-377457, 1:1000; Santa Cruz, CA, USA), rabbit anti-human p-AKT polyclonal antibody (sc-135650, 1: 800; Santa, Cruz, CA, USA), mouse an-

ti-human SRC monoclonal antibody (sc-32789, 1: 1000; Santa Cruz, CA, USA), Rabbit anti-human p-SRC polyclonal antibody (catalogue 2979, 1:800; Cell Signaling Technology, MA, USA), rabbit anti-human P38 polyclonal antibody (catalogue 9212, 1: 800; Cell Signaling Technology, MA, USA), rabbit anti-human p-P38 polyclonal antibody (catalogue 9211, 1: 2000; Cell Signaling Technology, MA, USA), rabbit anti-human ERK polyclonal antibody (ab17942, 1:1000; Abcam, MA, USA), rabbit anti-human p-ERK polyclonal antibody (ab131438, 1:800; Abcam, MA, USA), mouse anti-human JNK monoclonal antibody (sc-7345, 1:2000; Santa Cruz, CA, USA), mouse anti-human p-JNK monoclonal antibody (sc-81502, 1: 1000; Santa Cruz, CA, USA) and mouse anti-human GAPDH monoclonal antibody (MB001; 1:1000; Bioworld Technology Inc., China), respectively, and incubated in 4°C for overnight. The membranes were rinsed with TBST for 3 times, 10 min each time. Then secondary goat anti-rabbit or anti-mouse IgG-HRP antibodies (catalogue number AP201, AP503R, respectively; 1:5000; Bioworld Technology Inc., China) were added for incubation in room temperature for 2 h. The membranes were rinsed with TBST for 3 times, and 10 min per time. Then the membranes were developed with ECL (Beijing Kangwei Biotech, China) and taken photos to analyze the relative expression of proteins with GAPDH as internal referral.

Statistical analysis

The data were expressed as mean±SD and analyzed with software of SPSS17.0. Comparison between 2 groups was performed with t-test for independent samples and comparison for multiple groups was performed with one-way ANOVA following LSD (equal variances) or Dunnett's t-test (unequal variances). P<0.05 was set as significant level.

Results

Effects of different dosages of YCR on the apoptosis of A549 cells

The results of flow cytometry indicated that YCR induced apoptosis of A549 cells with a concentration-dependent manner from 0 to 12 mg/ml (Figure 1A-D). The apoptosis rate of A549 at 0, 4, 8 and 12 mg/ml YCR was 0.7%, 4.6%, 17.85 and 28.7%, respectively. YCR at 4 mg/ml had no obvious effect on the cell apoptosis and was chosen for subsequent experiments.

Effects of hypoxia and YCR on the cell morphology

Under microscopy, the A549 cells changed the morphology from oblate fusiform-shaped epithelial cells (Figure 2A) to elongated spindle-shaped mesenchymal cells after 72 h treatment with 2% O₂ (Figure

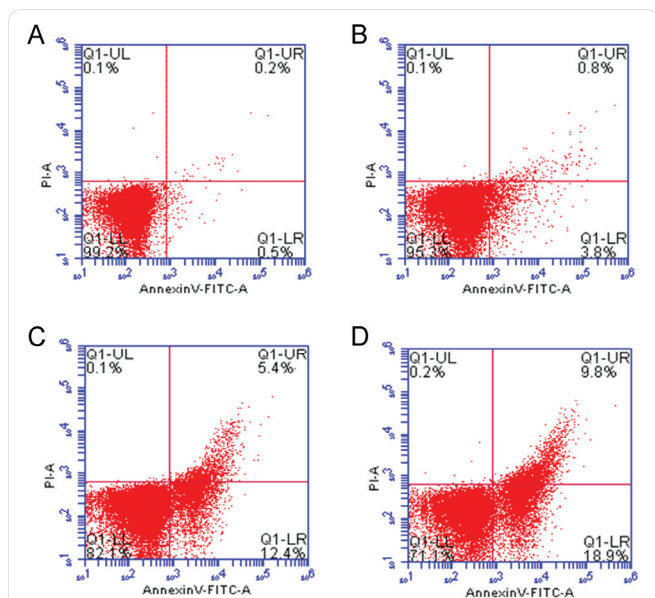


Figure 1. Effects of different concentrations of YCR on the apoptosis of A549 cells. A, Effects of Control group on the A549 cells apoptosis; B, Effects of 4 mg/ml YCR group on the A549 cells apoptosis; C, Effects of 8 mg/ml YCR group on the A549 cells apoptosis; D, Effects of 12 mg/ml YCR group on the A549 cells apoptosis. The cells were stained with Annexin V and PI, then the cells were incubated in dark for 10 min and examined by using the flow cytometry assay. Q1-UL represents the “Upper Left” quadrant; Q1-UR represents the “Upper Right” quadrant; Q1-LL represents “Lower Left” quadrant; Q1-LR represents the “Lower Right” quadrant. The percentage of the stained cell amounts were listed in every quadrant.

2B). After addition of YCR (4 mg/ml, 2% O₂ 72h), the morphological change of A549 cells was obviously alleviated (Figure 2C).

Effects of YCR on the expression of EMT-related genes

The real-time quantitative fluorescent PCR showed that the expression of EMT related genes including Snail1, Snail2, Twist, ZEB1 and ZEB2 were increased under hypoxic condition (2% O₂ 72 h), and there was significant differences when compared to that of control group (Table 2, *P*<0.05). The increased expression of Snail1, Snail2, Twist1, ZEB1 and ZEB2 by hypoxia (2% O₂ 72 h) was attenuated by YCR (4 mg/ml, 2% O₂ 72 h) and there was significant difference when compared to that in hypoxia group (2% O₂ 72 h) (*p*<0.05; Table 2). However, our preliminary experiments results showed that YCR can’t affect the gene expression under the normal oxygen condition (Data not shown).

Effects of YCR on the expression of EMT-related proteins

Under hypoxic condition (2% O₂ 72 h), the expres-

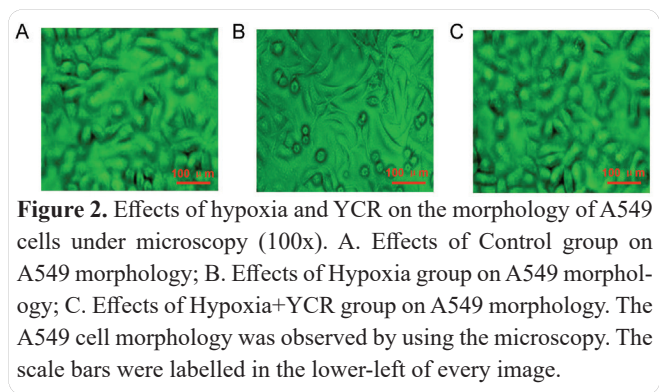


Figure 2. Effects of hypoxia and YCR on the morphology of A549 cells under microscopy (100x). A. Effects of Control group on A549 morphology; B. Effects of Hypoxia group on A549 morphology; C. Effects of Hypoxia+YCR group on A549 morphology. The A549 cell morphology was observed by using the microscopy. The scale bars were labelled in the lower-left of every image.

sion of E-cadherin protein representing epithelial phenotype in A549 cells was decreased and there was significant difference when compared to that in control group (*p*<0.05; Figure 3, Table 3). Meanwhile, the expression of vimentin and fibronectin proteins representing mesenchymal phenotype was increased and there was significant difference when compared to that in control group (*p*<0.05; Figure 3, Table 3). The treatment with YCR attenuated the changes induced by hypoxia. The expression of protein E-cadherin in hypoxia+YCR group (4 mg/ml, 2% O₂ 72 h) was increased while the expression of vimentin and fibronectin was decreased when compared to that in hypoxia group (2% O₂ 72 h), and there was significant difference between these 2 groups (*p*<0.05; Figure 3, Table 3).

In addition, the expression of proteins GRP78, smad2/3, p-smad2/3, SRC, p-SRC, P38, p-P38, ERK, p-ERK, JNK and p-JNK in A549 cells were also increased in hypoxic condition (2% O₂ 72h), and there was significant difference when compared to control group (*p*<0.05; Figure 3, Table 3). However, the expression of proteins PI3K, p-PI3K, AKT and p-AKT were not increased by hypoxia (2% O₂ 72h) when compared to that in control group (*p*>0.05; Figure 3, Table 3). In hypoxia+YCR group (4 mg/ml, 2% O₂ 72 h), the expression of proteins GRP78, smad2/3, p-smad2/3, SRC, p-SRC, PI3K, p-PI3K, AKT, p-AKT, P38, p-P38, ERK, p-ERK, JNK and p-JNK was decreased and there was significant difference when compared to that in hypoxia group (2% O₂ 72 h) (*p*<0.05; Figure 3, Table 3).

Discussion

The present study indicated that hypoxia induced human lung carcinoma cell A549 to transit from oblate fusiform-shaped epithelial cells to elongated spindle-shaped mesenchymal cells. Real-time fluorescence quantitative PCR indicated that the EMT-related genes were increased under hypoxia. Western blot results indicated that E-cadherin protein representing epithelial phenotype was increased while vimentin and fibronectin

Table 2. Expression of EMT-related genes in different groups (mean ±SD).

Gene	Control group	Hypoxia group	Hypoxia+YCR	F value	P value
Snail1	1.00±0.01	4.83±0.03*	1.37±0.04#	14869.99	0.000
Snail2	1.00±0.00	4.80±0.11*	1.50±0.16#	1020.707	0.000
Twist	1.00±0.00	4.81±0.16*	1.46±0.05#	1365.563	0.000
ZEB1	1.00±0.01	4.77±0.19*	1.29±0.23#	457.314	0.000
ZEB2	1.00±0.01	4.76±0.06*	1.46±0.09#	2990.93	0.000

Note: * *P*<0.01 vs control group; # *P*<0.01 vs hypoxia group.

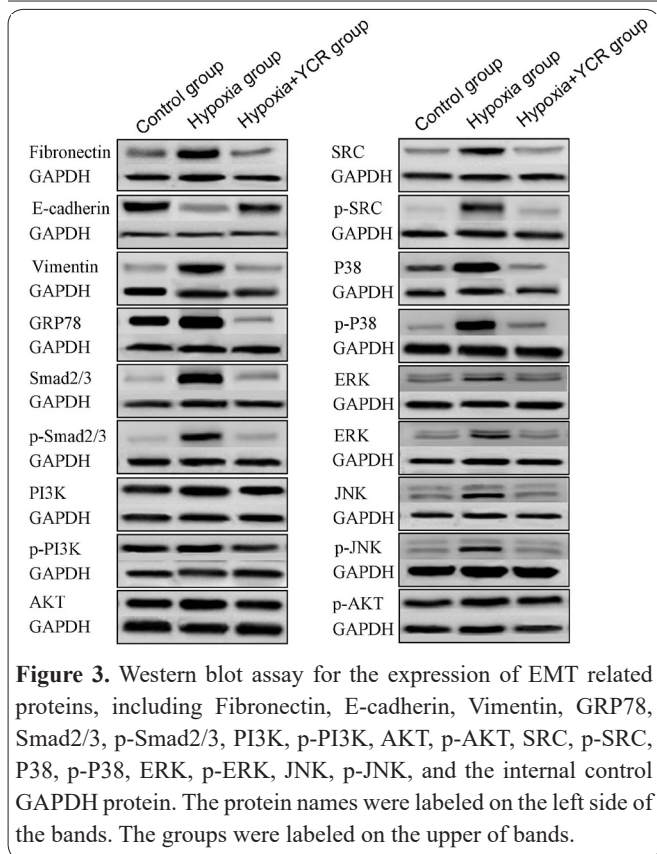


Figure 3. Western blot assay for the expression of EMT related proteins, including Fibronectin, E-cadherin, Vimentin, GRP78, Smad2/3, p-Smad2/3, PI3K, p-PI3K, AKT, p-AKT, SRC, p-SRC, P38, p-P38, ERK, p-ERK, JNK, p-JNK, and the internal control GAPDH protein. The protein names were labeled on the left side of the bands. The groups were labeled on the upper of bands.

tion proteins representing mesenchymal phenotype were increased. Furthermore, the EMT-related proteins GRP78, smad2/3, p-smad2/3, PI3K, p-PI3K, AKT, p-AKT, SRC, p-SRC, P38, p-P38, ERK, p-ERK, JNK and p-JNK were also increased by hypoxia. These changes induced by hypoxia were blocked by treatment with YCR. These results suggested that hypoxia induced EMT of A549 cells and YCR could block the EMT induced by hypoxia, possibly, through GRP78/SRC/ MAPK signal pathway.

EMT is a biological process that epithelial cells

transform to cells with mesenchymal phenotype through special mechanism (3). EMT can result in loss of the polarity of tumor cells, weaken the intercellular junction and make the cells incompact, which attributes to stronger invasive and migrating capacities for tumor cells and therefore provides favorable conditions for tumor metastasis (10). The inductive factors for EMT derive from extracellular stimulation, i.e., EMT is determined by the surrounding signaling factors such as cytokines, hypoxia and ischemia. Hypoxia is currently considered as an important factor for EMT and tumor metastasis (4,11). Consistently, the present study indicated that human lung carcinoma cell A549 demonstrated EMT in morphology under hypoxia.

MAPK members including JNK, P38 and ERK can upregulate snail, decrease the expression of E-cadherin and promote EMT and metastasis (12,13). Previous studies indicated that the signal pathways involved in hypoxia-induced EMT including p38MAPK in prostate cancer (14) and ERK in breast cancer (15), which are consistent with the present study that the expression of p38, ERK and p-ERK were increased in A549 cells under hypoxia. GRP78 is one member of the hot shock protein 70 family, plays key role in endoplasmic reticulum (ER), is significantly increased during ER stress and, therefore, is often used as biomarker for ER stress (16). Furthermore, the ER stress in tumor cells is closely correlated with EMT and the microenvironment of tumor can stimulate the ER stress and mediate the occurrence of EMT (17,18). Previous studies (19-21) indicated that smad2/3 and SRC/MAPK signals are involved in EMT through translocation to cellular nuclei to correlate with transcriptional factor snail and to inhibit the expression of E-cadherin. SRC can be involved in EMT through phosphorylation of cytoskeleton and adhesive structure to induce cell migration, activation of MAPK signal to produce reduction of intercellular junction, promotion of matrix degradation and increase of tumor invasive

Table 3. Expression of EMT related proteins in different groups (mean ±SD).

Gene	Control group	Hypoxia group	Hypoxia+YCR	F value	P value
Fibronectin	0.40±0.18	0.89±0.05*	0.31±0.04#	24.03	0.001
E-cadherin	0.77±0.12	0.26±0.04*	0.45±0.07#	29.767	0.001
Vimentin	0.31±0.04	0.77±0.12*	0.29±0.16#	15.837	0.004
GRP78	0.55±0.07	1.14±0.14*	0.23±0.13#	47.187	0.000
smad2/3	0.32±0.08	0.67±0.11*	0.35±0.11#	10.950	0.010
p-Smad2/3	0.17±0.07	0.47±0.11*	0.20±0.07#	11.888	0.008
PI3K	0.51±0.15	0.68±0.11 [§]	0.31±0.05#	8.202	0.019
p-PI3K	0.31±0.06	0.36±0.10 [§]	0.17±0.06#	5.413	0.045
AKT	0.77±0.10	0.83±0.12 [§]	0.54±0.07#	7.064	0.026
p-AKT	0.37±0.17	0.59±0.07 [§]	0.21±0.06#	8.369	.0180
SRC	0.29±0.04	0.51±0.12*	0.27±0.09#	6.984	0.027
p-SRC	0.19±0.06	0.43±0.13*	0.13±0.03#	10.311	0.011
P38	0.29±0.13	0.98±0.19*	0.31±0.08#	22.670	0.002
p-P38	0.14±0.06	0.48±0.14*	0.17±0.05#	12.126	0.008
ERK	0.29±0.05	0.59±0.11*	0.28±0.09#	10.809	0.010
p-ERK	0.17±0.05	0.35±0.10*	0.18±0.05#	5.976	0.037
JNK	0.33±0.15	0.71±0.05*	0.33±0.12#	11.131	0.010
p-JNK	0.23±0.13	0.53±0.11*	0.21±0.02#	9.510	0.014

Note: *P<0.05 vs control group; [§]P>0.05 vs control group; #P<0.05 vs hypoxia group.

capacity (22). Consistently, we found that the expression of GRP78, smad2/3, p-smad2/3, SRC, p-SRC, JNK and p-JNK was increased by hypoxia, suggesting hypoxia activates these signaling to be involved in the EMT in human lung tumor A549 cells. However, the expression of PI3K, p-PI3K, AKT and p-AKT was not significantly changed by hypoxia, suggesting these signals play no important role in the EMT of lung carcinoma under hypoxia.

Modulating the tumor microenvironment is one advantage of TCM in antitumor mechanism and increasing studies indicated that TCM is a potential approach to treat tumors by inhibiting EMT through snail/E-cadherin signal (23-25). YCR is an experiential recipe used in the Department of Tumor in the hospital to treat lung carcinoma and showed good clinical effects (2), however the mechanism is not clear. In the present study, we found that YCR inhibited the phenotype change of A549 cells from epithelial morphology to mesenchymal morphology and significantly attenuated the changes of E-cadherin, vimentin and fibronectin induced by hypoxia, suggesting that YCR can inhibit the EMT of A549 cells induced by hypoxia. Furthermore, we found that YCR blocked the change of EMT-related genes and proteins expression in A549 cells induced by hypoxia. These results suggest that YCR may play its anti-tumor effect in human lung carcinoma through modulating these signals including GRP78, SRC, MAPK, Smad and Snail pathways, and, therefore, provides evidence for the potential application of YCR in clinic treating tumors.

The previous study (7) also proved that the YCR could inhibit the hypoxia induced EMT by down-regulating the P4HB mRNA expression in A549 cells. Though this study (7) discovered the inhibition effects of YCR on the hypoxia induced EMT, however, this study only clarified by activating the P4HB mRNA expression. In the present study, we proved for the first time that YCR inhibits the EMT by activating GRP78, Smad2/3 and SRC/MAPK signaling pathway. Therefore, we think that our study added some novel data for the function of YCR in the EMT.

However, the detailed mechanism is unclear and remains to be further studied. In the future study, we will apply gene silencing techniques and specific protein inhibitors to study the specific signal involved in the inhibition of EMT by YCR in hypoxic condition.

Acknowledgements

The study was supported by the National Science Foundation of China (NO.81273963) and Provincial National Science Foundation of Guangdong (NO. S2012020010886).

References

- Sennoune, S.R., Arutunyan, A., del Rosario, C., Castro-Marin, R., Hussain, F., Martinez-Zaguilan, R., V-ATPase regulates communication between microvascular endothelial cells and metastatic cells. *Cell Mol Biol (Noisy-le-grand)* 2014, **60**: 19-25.
- Xu, L., Zhang, Y., Wang, H., Zhang, G., Ding, Y., Zhao, L., Tumor suppressor miR-1 restrains epithelial-mesenchymal transition and metastasis of colorectal carcinoma via the MAPK and PI3K/AKT pathway. *J Transl Med* 2014; **12**: 244. doi: 10.1186/s12967-

- 014-0244-8.
- Lee, Y., Lee, M., Kim, S., Gas6 induces cancer cell migration and epithelial-mesenchymal transition through upregulation of MAPK and slug. *Biochem Biophys Res Commun* 2013; **434**: 8-14. doi: 10.1016/j.bbrc.2013.03.082.
- Liu, L., Chen, X., Wang, Q., Qu, Z., Lu, Q., Zhao, J., Yan, X., Zhang, H., Zhou, Y., Notch3 is important for TGF-beta-induced epithelial-mesenchymal transition in non-small cell lung cancer bone metastasis by regulating ZEB-1. *Cancer Gene Ther* 2014; **21**: 364-372. doi: 10.1038/cgt.2014.39.
- Ling, C.Q., Yue, X.Q., Ling, C., Three advantages of using traditional Chinese medicine to prevent and treat tumor. *J Integr Med* 2014; **12**: 331-335. doi: 10.1016/S2095-4964(14)60038-8.
- Hu, B., Wang, S.S., Du, Q., Traditional Chinese medicine for prevention and treatment of hepatocarcinoma: From bench to bedside. *World J Hepatol* 2015, **7**: 1209-1232. doi: 10.4254/wjh.v7.i9.1209.
- Sun, L.L., Lin, L.Z., Effects of YiQi Huatan Decoction on epithelial-mesenchymal transition and P4HB expression in A549 cells under hypoxia microenvironment. *Trad Chin Drug Res Clin Pharmacol* 2013; **24**: 454-457. doi: 10.3969/j.issn.1003-9783.2013.05.006.
- Lin, L.Z., Wang, S.M., Zhou, J.X., Effects of yiqi chutan recipe on tumor growth, survival time and expressions of PRDX-1 and PRDX-6 in Lewis lung carcinoma model mice with pi-deficiency syndrome. *Zhongguo Zhong Yi Jie He Ze Zhi* 2011; **31**: 99-103.
- Kokkinos, M.I., Wafai, R., Wong, M.K., Newgreen, D.F., Thompson, E.W., Waltham, M., Vimentin and epithelial-mesenchymal transition in human breast cancer--observations in vitro and in vivo. *Cells Tissues Organs* 2007, **185**: 191-203.
- Christofori, G., New signals from the invasive front. *Nature* 2006, **441**: 444-450.
- Liu, N., Wang, Y., Zhou, Y., Pang, H., Zhou, J., Qian, P., Liu, L., Zhang, H., Kruppel-like factor 8 involved in hypoxia promotes the invasion and metastasis of gastric cancer via epithelial to mesenchymal transition. *Oncol Rep* 2014; **32**: 2397-2404. doi: 10.3892/or.2014.3495.
- Bellovin, D.I., Bates, R.C., Muzikansky, A., Rimm, D.L., Mercurio, A.M., Altered localization of p120 catenin during epithelial to mesenchymal transition of colon carcinoma is prognostic for aggressive disease. *Cancer Res* 2005, **65**: 10938-10945.
- Mulholland, D.J., Kobayashi, N., Ruscetti, M., Zhi A., Tran, L.M., Huang, J., Gleave, M., Wu, H., Pten loss and RAS/MAPK activation cooperate to promote EMT and metastasis initiated from prostate cancer stem/progenitor cells. *Cancer Res* 2012; **72**: 1878-1889. doi: 10.1158/0008-5472.CAN-11-3132.
- Cho, K.H., Choi, M.J., Jeong, K.J., Kim, J.J., Hwang, M.H., Shin, S.C., Park, C.G., Lee, H.Y., A ROS/STAT3/HIF-1 α signaling cascade mediates EGF-induced TWIST1 expression and prostate cancer cell invasion. *Prostate* 2014, **74**: 528-536. doi: 10.1002/pros.22776.
- Ren, T., Zhang, W., Liu, X., Zhao, H., Zhang, J., Zhang, J., Li, X., Zhang, Y., Bu, X., Shi, M., Yao, L., Su, J., Discoidin domain receptor 2 (DDR2) promotes breast cancer cell metastasis and the mechanism implicates epithelial-mesenchymal transition programme under hypoxia. *J Pathol* 2014, **234**: 526-537. doi: 10.1002/path.4415.
- Lee, E., Nichols, P., Spicer, D., Groshen, S., Yu, M.C., Lee, A.S., GRP78 as a novel predictor of responsiveness to chemotherapy in breast cancer. *Cancer Res* 2006, **66**: 7849-7853.
- Lane, D.J., Mills, T.M., Shafie, N.H., Merlot, A.M., Saleh Moussa, R., Kalinowski, D.S., Kovacevic, Z., Richardson, D.R., Expanding horizons in iron chelation and the treatment of cancer: role of iron in the regulation of ER stress and the epithelial-mesenchymal transition. *Biochem Biophys Acta* 2014; **1845**: 166-181. doi: 10.1016/j.bbcan.2014.01.005.
- Ulianich, L., Garbi, C., Treglia, A.S., Punzi, D., Miele, C., Raciti, G.A., Beguinot, F., Consiglio, E., Di Jeso, B., ER stress is

associated with dedifferentiation and an epithelial -to-mesenchymal transition-like phenotype in PC C13 thyroid cells. *J Cell Sci* 2008, **121**: 477-486. doi: 10.1242/jcs.017202.

20. Bianchi, A., Gervasi, M.E., Bakin, A., Role of $\beta 5$ -integrin in epithelial-mesenchymal transition in response to TGF- β . *Cell Cycle* 2010, **9**: 1647-1659.

21. Kumar, K.J., Vani, M.G., Chueh, P.J., Mau, J.L., Wang, S.Y., Antrodin C inhibits epithelial-to-mesenchymal transition and metastasis of breast cancer cells via suppression of Smad2/3 and beta-catenin signaling pathways. *PLoS One* 2015; **10**: e0117111. doi: 10.1371/journal.pone.0117111.

22. Bokobza, S.M., Ye, L., Kynaston, H., Jiang, W.G., Growth and differentiation factor 9 (GDF-9) induces epithelial-mesenchymal transition in prostate cancer cells. *Mol Cell Biochem* 2011, **49**: 33-

40. doi: 10.1007/s11010-010-0657-5.

23. Nagathihalli, N.S., Merchant, N.B., Src-mediated regulation of E-cadherin and EMT in pancreatic cancer. *Front Biosci (Landmark Ed)* 2012; **17**: 2059-2069.

24. Kin, R., Kato, S., Kaneto, N., Sakurai, H., Hayakawa, Y., Li, F., Tanaka, K., Saiki, I., Yokoyama, S., Procyanidin C1 from Cinnamon Cortex inhibits TGF- β -induced epithelial-to-mesenchymal transition in the A549 lung cancer cell line. *Int J Oncol* 2013, **43**: 1901-1906. doi: 10.3892/ijo.2013.2139.

25. Ji, Q., Liu, X., Han, Z., Zhou, L., Sui, H., Yan, L., Jiang, H., Ren, J., Cai, J., Li, Q., Resveratrol suppresses epithelial-to-mesenchymal transition in colorectal cancer through TGF-beta1/Smads signaling pathway mediated Snail/E-cadherin expression. *BMC Cancer* 2015; **15**: 97. doi: 10.1186/s12885-015-1119-y.